Immunity
Article

Identification and Characterization of Enhancers Controlling the Inflammatory Gene Expression Program in Macrophages

Serena Ghisletti,[1,5] Iros Barozzi,[1,5] Flore Mietton,[1,5] Sara Polletti,[1,5] Francesca De Santa,[1] Elisa Venturini,[2] Lorna Gregory,[3] Lorne Lonie,[3] Adeline Chew,[4] Chia-Lin Wei,[4] Jiannis Ragoussis,[3] and Gioacchino Natoli[1,*]
[1]Department of Experimental Oncology, European Institute of Oncology (IEO), IFOM-IEO Campus, Via Adamello 16, 20139 Milan, Italy
[2]Consortium for Genomic Technologies (Cogentech), IFOM-IEO Campus, I-20135 Milan, Italy
[3]Genomics Laboratory, Wellcome Trust Centre for Human Genetics (WTCHG), University of Oxford, Oxford OX3 7BN, UK
[4]Genome Technology & Biology Group, Genome Institute of Singapore, 60 Biopolis Street #02-01, Singapore 138672, Republic of Singapore
[5]These authors contributed equally to this work
*Correspondence: gioacchino.natoli@ifom-ieo-campus.it
DOI 10.1016/j.immuni.2010.02.008

SUMMARY

Enhancers determine tissue-specific gene expression programs. Enhancers are marked by high histone H3 lysine 4 mono-methylation (H3K4me1) and by the acetyl-transferase p300, which has allowed genome-wide enhancer identification. However, the regulatory principles by which subsets of enhancers become active in specific developmental and/or environmental contexts are unknown. We exploited inducible p300 binding to chromatin to identify, and then mechanistically dissect, enhancers controlling endotoxin-stimulated gene expression in macrophages. In these enhancers, binding sites for the lineage-restricted and constitutive Ets protein PU.1 coexisted with those for ubiquitous stress-inducible transcription factors such as NF-κB, IRF, and AP-1. PU.1 was required for maintaining H3K4me1 at macrophage-specific enhancers. Reciprocally, ectopic expression of PU.1 reactivated these enhancers in fibroblasts. Thus, the combinatorial assembly of tissue- and signal-specific transcription factors determines the activity of a distinct group of enhancers. We suggest that this may represent a general paradigm in tissue-restricted and stimulus-responsive gene regulation.

INTRODUCTION

The vastness and complexity of mammalian genomes is a major hurdle toward a systematic identification of *cis*-regulatory regions. Technological progresses in the identification of transcription start sites (TSS) have improved our ability to locate promoters (Carninci et al., 2006). Conversely, identification of distant gene regulatory sequences has until recently almost exclusively relied on comparative genomics and specifically on the identification of evolutionarily conserved extra- and intragenic noncoding sequences (Boffelli et al., 2003; Prabhakar et al., 2006). Comparative approaches to enhancer mapping successfully led to the identification of many functional enhancers, which included several ultraconserved elements (Pennacchio et al., 2006; Visel et al., 2008), namely short extragenic regions identical between the human and rodent genomes (Bejerano et al., 2004; Katzman et al., 2007). However, these approaches suffer from important limitations; for instance, regulatory sequences controlling environmental responses (like immune response to pathogens and stress responses in general) evolved rapidly together with the associated genes (which underwent frequent duplications and losses) (Ponting, 2008). Therefore, although regulatory sequences controlling developmental genes tend to be highly conserved, those associated with environmental genes are believed to be less evolutionarily constrained. Overall, a sizable fraction of functional noncoding sequences involved in gene regulation are lineage specific and not particularly conserved across mammals (Birney et al., 2007). Moreover, evolutionary conservation does not allow predicting in which tissue(s) or condition(s) a given enhancer is active (Visel et al., 2009). A major advance toward systematic enhancer mapping has been the identification of a specific enhancer-associated chromatin signature consisting in a broad (several kilobases-long) domain of histone H3K4 monomethylation (H3K4me1) combined with low amounts of H3K4me3 (a modification associated with the TSSs of active or poised genes) (Heintzman et al., 2007). H3K4me1^{hi}/H3K4me3^{lo} domains are also frequently bound by the histone acetyltransferase and transcriptional coregulator p300 (Heintzman et al., 2007). Because p300-bound regions within H3K4me1^{hi}/H3K4me3^{lo} domains are narrow, they are particularly useful in spotting core enhancer sequences (Heintzman et al., 2009; Visel et al., 2009). In spite of these progresses, our current understanding of the genomic determinants of enhancer activity and of how enhancers become functional in specific cellular and/or environmental contexts is still rudimentary and can be summarized in the broad concept that enhancers contain heterotypic clusters of transcription factor binding sites (TFBSs) that work in a cell-type-specific fashion.

The objective of this study was to determine the regulatory logic of a discrete set of enhancers involved in a paradigmatic context-dependent environmental response, endotoxin-induced gene activation in macrophages. Innate immune responses to

microbes involve complex gene expression programs that are activated both in professional innate immune cells such as neutrophils and macrophages and tissue cells coming in contact with microbes. Although genes induced in response to microbial challenge in professional and nonprofessional innate immune cells extensively overlap, there are important qualitative and quantitative differences. For instance, production of the T helper 1 (Th1) cell-polarizing cytokine IL-12 is restricted to macrophages and dendritic cells, even though this gene depends on an NF-κB protein (cRel) (Sanjabi et al., 2000) that is expressed in other immune (B and T lymphocytes) and nonimmune cells (e.g., fibroblasts) (Hayden et al., 2006). The gene encoding TNF-α, a major mediator of inflammation, is expressed by several cell types but at amounts that are orders of magnitude lower than those found in macrophages (Tracey and Cerami, 1994). Therefore, although it is clear that the cellular context strongly impacts on the inflammatory gene expression program (and on stress responses in general), the underlying mechanisms are largely ignored.

The data we obtained demonstrate that a common occurrence in endotoxin-activated enhancers in macrophages is the heterotypic clustering of functional binding sites for one or more cell-type-restricted and constitutive TFs (which provide context-dependence) and ubiquitous stress-inducible TFs (which enable responsiveness to environmental stimuli). These data enhance our understanding of the mechanisms controlling inflammatory responses at the transcriptional level and may suggest a general paradigm of how context-dependent inducible gene expression programs are encoded in the underlying genome.

RESULTS

Inducible Binding of p300 to Enhancers Activated by Inflammatory Stimuli

Given that enhancers were previously found to be constitutively associated with both p300 and the H3K4me1^{hi}/H3K4me3^{lo} signature in the cell types and experimental conditions analyzed (Heintzman et al., 2009), we investigated by chromatin immunoprecipitation (ChIP) whether lipopolysaccharide (LPS) stimulation affects p300 binding and/or H3K4me1 association at a well-characterized intronic enhancer controlling inducible expression of *Sod2* (encoding the manganese superoxide dismutase) (Jones et al., 1997). Although the intronic *Sod2* enhancer was constitutively associated with H3K4me1, it recruited p300 only in response to LPS stimulation (Figure 1A). LPS-induced binding of the NF-κB subunit p65, an essential regulator of inflammatory gene expression (Hayden et al., 2006), paralleled p300 recruitment. Therefore, we exploited the inducible binding of p300 to chromatin to identify putative *cis*-regulatory regions involved in LPS-stimulated gene expression. Anti-p300 ChIP was carried out on formaldehyde-crosslinked chromatin obtained from untreated and LPS-treated (2 hr) bone marrow-derived mouse macrophages and immunoprecipitated DNA was subjected to massively parallel sequencing. We detected 2742 peaks ("inducible peaks"; Table S1 available online) that were increased by LPS stimulation at high statistical significance ($p < 10^{-6}$; see Experimental Procedures). A small fraction of these peaks (310/2742; 11.3%) was already detectable in unstimulated macrophages, but the majority of them (2432/2742; 88.7%) appeared only after treatment. We also detected 8064 p300 peaks in untreated macrophages, which were not increased by LPS treatment ("noninducible" peaks; Table S1). Validation by standard ChIP and quantitative PCR (ChIP-QPCR) of random peaks with a broad range of associated p values confirmed the sequencing results in both groups (Figure S1). The distribution of inducible p300 peaks relative to genes in the University of California Santa Cruz (UCSC) Known Genes data set was consistent with previous reports (Heintzman et al., 2009; Visel et al., 2009), with a strong representation of intergenic and intronic sequences (56% and 27% respectively; Figure 1B). Twenty-nine percent of extragenic peaks were located within 20 kb from annotated TSS and 73% were within 100 kb (Figure 1B). The intragenic peaks were often close to the TSS (44% within 20 kb), consistent with the common occurrence of enhancers in introns at the 5′ of genes, but a large fraction of them was located at much larger distances. The 392 inducible p300 peaks associated with promoters and adjacent regions (±2.5 kb surrounding TSSs of UCSC known genes) were excluded from further analyses and our experimental data set of putative enhancers involved in LPS-induced gene expression eventually consisted in 2350 TSS-distal regions (1519 intergenic and 831 intragenic sequences).

Using publicly available microarray data, we first evaluated whether inducible p300 peaks are associated with genes whose expression is increased by LPS stimulation. To this aim, we tentatively assigned p300 peaks to individual genes. To reasonably limit arbitrariness in gene assignment, we considered only intragenic peaks between +2.5 and +20 kb and intergenic peaks located between −2.5 kb and −20 kb from a mapped TSS and we linked them to the corresponding genes. When compared to a control group consisting of all the RefSeq genes mappable to probes in the microarray, the set of genes associated with inducible p300 binding was enriched for LPS-stimulated transcripts at high statistical significance ($p < 10^{-16}$ in a chi-square test) (Figure 1C), thus providing initial correlative evidence that inducible binding of p300 marks regulatory regions associated with LPS-stimulated genes. Importantly, genes associated with enhancers bound by p300 in an LPS-inducible manner belonged to several classes of LPS-responsive genes (primary, secondary, promiscuously, and selectively activated genes) (Ramirez-Carrozzi et al., 2009), without any obvious specificity. Some representative regions are shown in Figure 1D, including the *Sod2* intronic enhancer, an intergenic region upstream of the genic cluster containing the tumor necrosis factor alpha (*Tnfa*) and the lymphotoxin alpha (*Lta*) genes, and the genomic region including the housekeeping beta-actin (*Actb*) gene, which contains only noninducible p300 peaks. Thus, inducible p300 binding can be used for mapping potential enhancers activated in response to macrophage stimulation.

Sites of Inducible p300 Binding Have an Enhancer-Associated Chromatin Signature

We next set out to determine whether the regions identified in the p300 ChIP-sequencing screening have properties of bona fide enhancers in terms of chromatin signature, sequence conservation, presence of functional TFBSs, and ability to drive macrophage-restricted LPS-inducible gene expression.

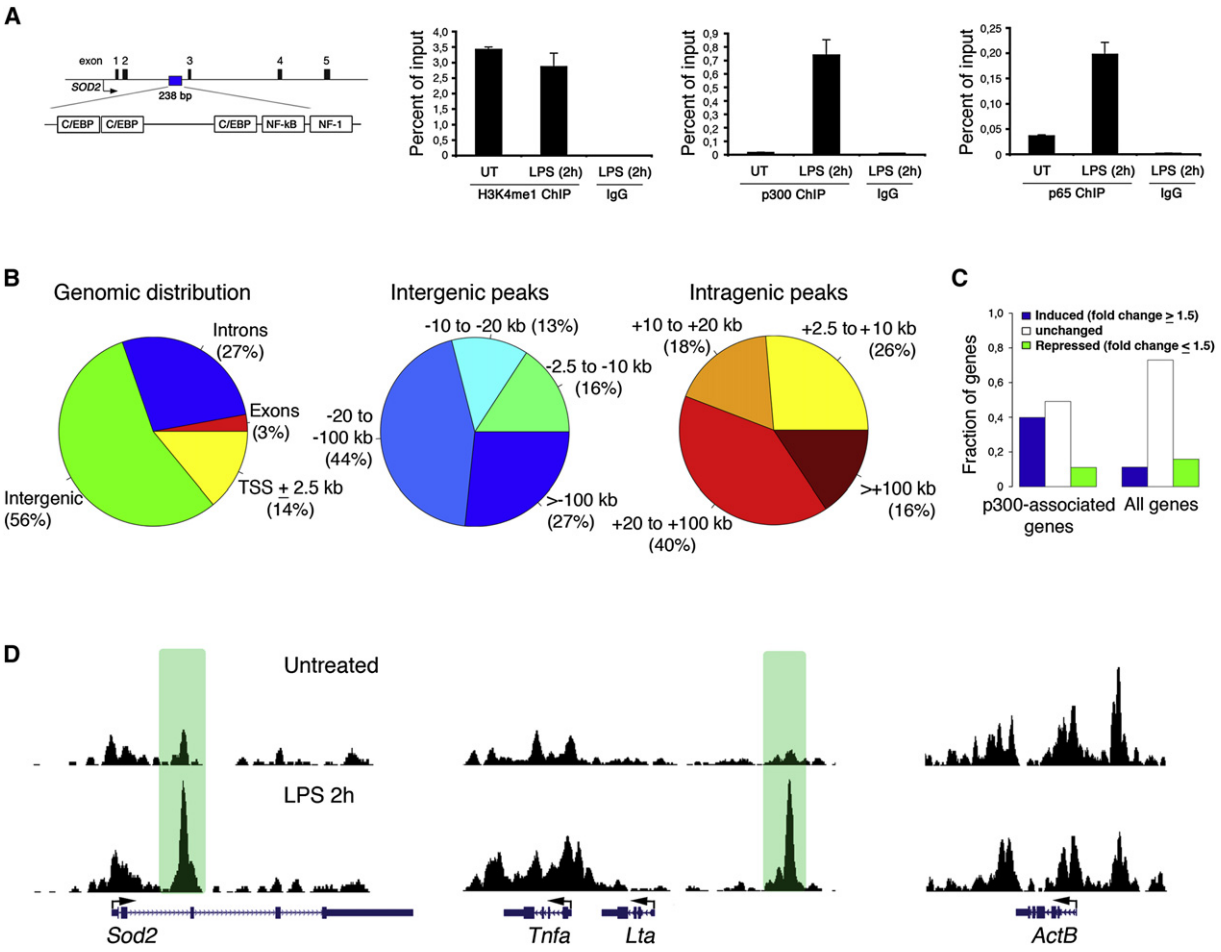

Figure 1. LPS Induces Binding of p300 to Potential Regulatory Sequences in Mouse Macrophages

(A) Inducible binding of p300 to the *Sod2* intronic enhancer in mouse macrophages. The position of the *Sod2* intronic enhancer is shown in the scheme together with the mapped TFBSs. ChIP was carried out with H3K4me1, p300, and p65 NF-kB antibodies. Data are expressed as percent of the input.

(B) Genomic distribution of LPS-inducible p300 peaks relative to UCSC known genes.

(C) Association of inducible p300 peaks with genes activated by LPS stimulation. Inducible p300 peaks between −2.5 and −20 kb and between +2.5 and +20kb from mapped TSSs were assigned to the associated genes. The fraction of these genes induced (fold change ≥ 1.5), unchanged, or repressed in response to LPS stimulation is shown. For comparison, a control set including all RefSeq genes in the microarray was used. The difference between the two groups is statistically significant ($p < 10^{-16}$).

(D) Raw p300 ChIP-Seq data at three representative genomic regions. Inducible p300 peaks are highlighted in green.

We first generated a data set of H3K4me1-associated sequences in unstimulated macrophages and cross-compared it to the inducible p300 data set and to an H3K4me3 data set we recently obtained in the same cellular system (De Santa et al., 2009). We also generated an H3K4me1 data set after LPS stimulation, but data were substantially identical to those obtained in unstimulated conditions, indicating a poor reactivity of this histone mark to environmental stimuli (data not shown). Distal p300 peaks were in most cases contained within H3K4me1^{hi}/H3K4me3^{lo} domains (Figure 2), thus suggesting that the chromatin environment surrounding regions of LPS-inducible p300 binding is similar to the one previously described in functional enhancers. Interestingly, the central sequences (~250–300 nt) within H3K4me1 regions (corresponding to the p300 peaks, around which these regions were aligned) were frequently depleted of H3K4me1, which may indicate selective nucleosome eviction (Figure 2 and Figure S2). Only a small fraction of inducible p300 peaks resided outside of H3K4me1^{hi}/H3K4me3^{lo} domains, a result in keeping with previous observations in transformed cell lines (Heintzman et al., 2007). Overall, distal regions bound by p300 in response to LPS stimulation were associated with the classical chromatin signature of enhancers.

Sequence Conservation and Ultraconservation at Inflammatory Enhancers

Regulatory elements within enhancers are subjected to purifying selection, even though a substantial fraction of regulatory DNA lacks detectable sequence constraints (Birney et al., 2007; Ponting, 2008). To determine the degree of conservation in the sequences bound by p300 in an inducible manner, we first scored the presence of stretches conserved across 20 placental mammalian genomes with the phastCons program (Siepel

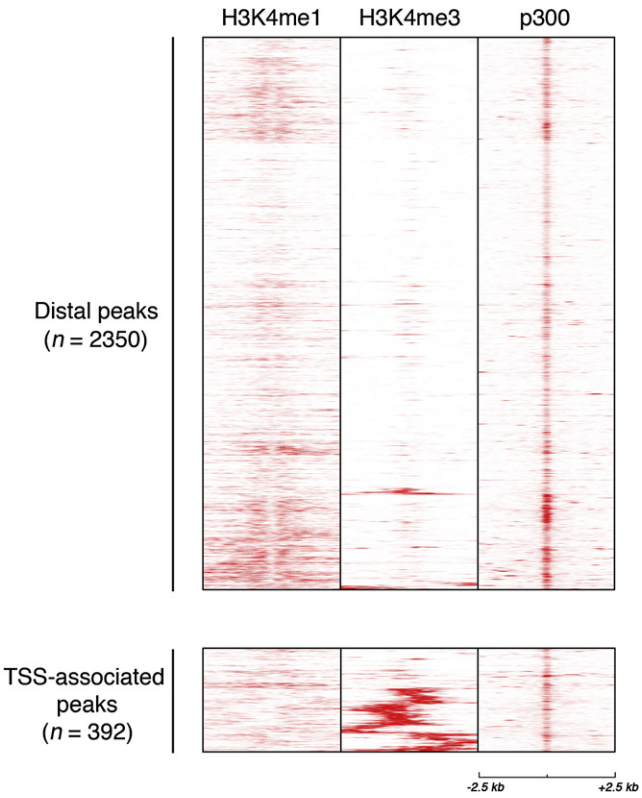

Figure 2. Inducible p300 Peaks Occur in Regions with a Chromatin Signature of Enhancers

H3K4me1 and H3K4me3 state at p300 peaks. ChIP-Sequencing data obtained with H3K4me1 and H3K4me3 antibodies in untreated macrophages were used for identifying the enhancer chromatin signature at LPS-inducible distal peaks. Each line represents a p300 peak. Regions (5 kb) were centered on the summit of the p300 peaks. The upper panel refers to the 2350 distal (intergenic and intragenic p300 peaks), whereas lower panel refers to the 392 inducible p300 peaks located ±2.5 kb from the TSSs of UCSC known genes.

et al., 2005), which detects sequence conservation in a fraction between 2.8% and 8.1% of the human genome (depending on the parameters used). This analysis (Figure 3A and Table S1) revealed that distal regions associated with inducible p300 binding contain sequence elements under evolutionary conservation. When considering 5 kb windows surrounding inducible p300 peaks, conserved elements were clearly clustered in the central regions, corresponding to the sequences contacted by p300 (Figure 3A). Association with evolutionary conserved sequence elements was statistically significant when compared to random genomic sets (Figure 3A, right panel). We next analyzed the correlation between high degree of sequence conservation and p300 binding using a database of 171,853 human-rodent highly conserved noncoding sequences (CNSs) (Prabhakar et al., 2006), corresponding to ~2.3% of the mouse genome. We found that 242/2350 (10.3%) inducible and distal p300 peaks overlapped these CNSs. To determine the statistical significance of this finding, we first calculated the overlap of inducible p300 peaks (Figure 3B, red line) with CNSs at different cutoffs of p values (Prabhakar et al., 2006). We then generated 1000 random sets of sequences with the same genomic composition and derived a distribution (boxes) of expected overlap values for each cutoff of CNSs p values. This way we calculated the probability (p) that the observed values are significantly different from the expected distribution. Association of inducible p300 peaks with CNSs was statistically significant ($p \leq 0.01$) for CNSs with cutoff values higher than a p value $\leq 10^{-10}$ (Figure 3B). It is important to notice that statistical significance is lost when elements with an extreme degree of evolutionary conservation (those at the right side of the graph) are considered. These ultraconserved elements, which are subjected to strong purifying selection (Katzman et al., 2007), frequently correspond to developmental enhancers (Visel et al., 2008), and it is reasonable to expect them not to be associated with environmental genes, whose evolution occurs on a much faster time scale than that of developmental genes (Ponting, 2008). Overall, LPS-inducible binding of p300 frequently occurs in regions of strong (but not extreme) evolutionary conservation. It is also clear that part of these putative enhancers lack CNSs, a result consistent with the known evolutionary properties and lineage specificity of environmental genes (Ponting, 2008).

Functional and Organizational Properties of Inflammatory Enhancers

We next functionally evaluated some genomic regions bound by p300 to determine whether they direct macrophage-specific inducible gene expression. A panel of randomly selected positive regions (corresponding to peaks with a broad range of p values) and two negative controls (regions not bound by p300) were cloned upstream of a minimal promoter driving luciferase expression and transfected in the macrophage cell line Raw264.7 and in two LPS-sensitive nonmyeloid mouse cell lines, the hepatoblastoma Hepa1-6, and the melanoma cell line C57/B1. The p300-bound regions tested (but not the negative control sequences) increased basal luciferase expression to a various extent (as compared to the enhancer-less vector) and provided responsiveness to LPS stimulation in Raw264.7 cells (Figure 4A). The same sequences were either inactive or much less active when transfected in the other two cell lines. Overall, the p300-bound regions identified in the ChIP-Seq screening have a chromatin signature, a degree of conservation and functional properties compatible with a role as macrophage-restricted enhancers involved in LPS-inducible gene expression. We therefore set out to investigate the underlying genomic determinants of their functional properties and specifically of their macrophage-restricted inducible activity.

If inducible p300 peaks correspond to enhancers controlling inflammatory gene expression, an obvious prediction is that they should be enriched for binding sites for stimulus-activated TFs required for the deployment of the inflammatory gene expression program, like NF-κB (Rel) and IRF family members (Taniguchi et al., 2001; Hayden and Ghosh, 2008). We searched for TFBS overrepresented in the p300 data set relative to two reference sets, namely a whole chromosome (mouse chr 19) and a set of the 5 kb sequences located upstream of the TSSs of all mouse RefSeq genes. We first assembled a library of DNA binding motifs consisting of the 138 position weight matrices (PWMs) in the Jaspar database (Sandelin et al., 2004) and 208 high quality PWMs (referring to 104 mouse TFs) recently obtained with protein-binding microarrays containing

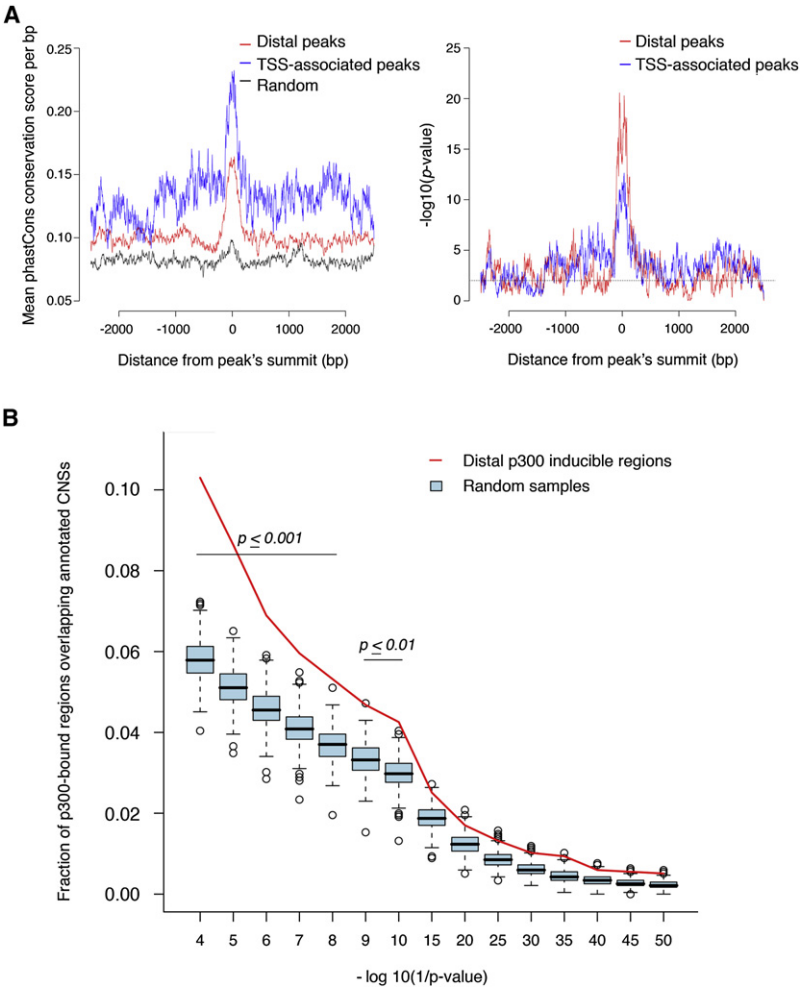

Figure 3. Sequence Conservation and Ultraconservation at Regions of Inducible p300 Binding

(A) Conserved sequence elements were analyzed with the phastCons program (Siepel et al., 2005). In the left panel, average conservation scores (phastCons score per bp) in the distal, TSS-associated and random groups are shown. Inducible p300 peaks were centered on their summit. As shown in the right panel, statistical significance of sequence conservation in the two groups was evaluated as compared to random sets. The y axis indicates the p value of the deviation from random. The horizontal gray line indicates the threshold for statistical significance (set to $p < 0.01$).

(B) Enrichment of inducible p300 peaks at previously annotated conserved noncoding sequences. A database of 171,853 human-rodent CNSs (Prabhakar et al., 2006) was overlapped with the 2350 inducible distal p300 peaks or with 1000 random sets composed of an identical number of sequences of similar length and composition. The fraction of p300 peaks (red line) and the distribution of random sequences (boxes) overlapping annotated CNSs ordered by increasing p values (according to Prabhakar et al., 2006) is shown. Association of p300 peaks with CNSs is highly statistically significant except when extremely constrained CNSs (right-half of the graph) are considered.

all possible 10 bp sequences (Badis et al., 2009). A total of 41 motifs were found to be enriched at a $p \leq 0.01$ as compared to both reference sets, including five matrices for NF-κB (Rel) proteins and four matrices for IRF proteins (Figure 4B and Table S2). Overall, 54% of the inducible p300 peaks scored positive for at least two NF-κB (Rel) PWMs and 48% were positive for at least two IRF PWMs. As predicted by previous data on transcriptional coregulation by NF-kB and IRFs (Doyle et al., 2002), binding sites for these two TFs co-occur at a subset of regulatory regions. Moreover, matrices for additional TFs known to regulate inflammatory gene expression (like FOS and AP-1) (Baud and Karin, 2001) or differentiation of the myeloid lineage (like MAFB and RUNX1 or AML1) (Kelly et al., 2000; Nagamura-Inoue et al., 2001) were retrieved (Figure 4B and Table S2). These data show that LPS-inducible p300 peaks clearly define a set of *cis*-regulatory sequences strongly enriched for inflammatory and macrophage-restricted TFs, demonstrating the efficiency of the ChIP-Seq screening we used at retrieving macrophage-specific inflammatory enhancers.

Probably the most striking finding of this analysis was that the most enriched TF in the data set was PU.1 (Sfpi1 or Spi1) and its closely related paralogue SpiB (identified by three different PWMs) (Figure 4B and Table S2). PU.1 is a hematopoietic TF required for the development of multiple lineages (including macrophages, neutrophils, and B and T cell lymphocytes) (Scott et al., 1994) and expressed at highest amounts in mature macrophages (high amounts of PU.1 favoring development of myeloid cells over alternative lineages) (Nerlov and Graf, 1998; DeKoter and Singh, 2000). PU.1 is required not only for macrophage differentiation but also for transcriptional control of inducible genes in mature macrophages (Eichbaum et al., 1994; Grove and Plumb, 1993; Nguyen and Benveniste, 2000). Interestingly, although IRF and NF-kB matrices generated well-defined clusters indicating discrete subgroups of enhancers, the PU.1 and SpiB matrices were broadly enriched all over the data set, suggesting that association of enhancers with PU.1 may be a rather common occurrence in macrophages. Regions of inducible p300 binding containing NF-kB or IRF PWMs very frequently contained associated PU.1 binding sites (76% and 78% overlap, respectively). ChIP-QPCR experiments demonstrated a strong, and most often constitutive, PU.1 binding to a panel of p300-bound distal sequences (Figure 4C), suggesting that sites identified in silico are in fact functional. Mutations of PU.1 binding sites abrogated both basal and inducible promoter activity in heterologous reporter assays, indicating that they are essential for enhancer functionality (Figure 4D).

The Hematopoietic Ets Family Transcription Factor PU.1 Marks Enhancers in Macrophages

To obtain a global view of PU.1 genomic distribution, we generated two PU.1 ChIP-Seq data sets in untreated and LPS-treated macrophages (2 hr stimulation). Using an extremely restrictive threshold of $p < 10^{-10}$, we detected 44,445 peaks in untreated

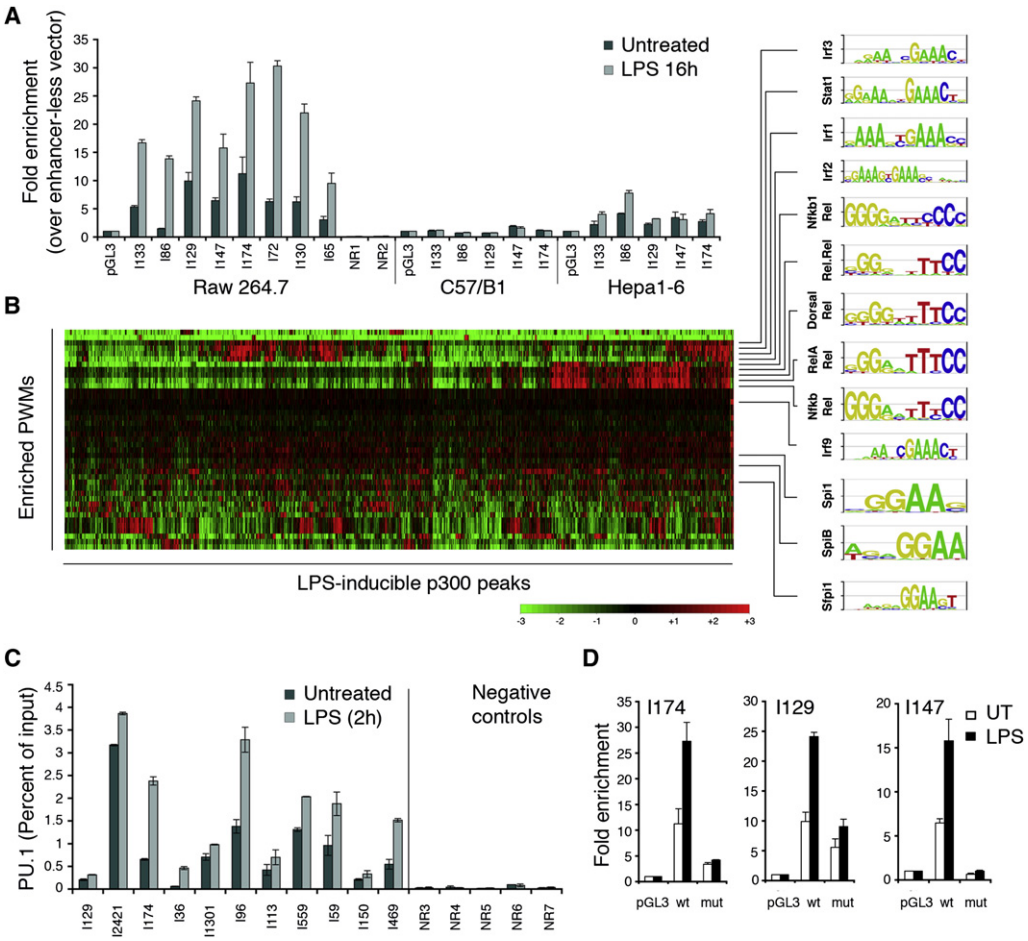

Figure 4. Regions of Inducible p300 Binding Are Macrophage-Specific Enhancers Containing Binding Sites for Inflammatory and Macrophage-Restricted TFs

(A) Functional assessment of a panel of p300-bound regions and two control regions (NR1 and NR2) with luciferase-based reporter assays in a macrophage cell line (Raw264.7), a hepatoblastoma line (Hepa1-6), and a melanoma line (C57/B1). Cells were either left untreated or stimulated with LPS for 16 hr before harvesting. pGL3 represents an enhancer-less cloning vector. Numbers on the x axis indicate the peak ID (according to Table S1).

(B) Enrichment for TFBS in the p300 data set. Each vertical column corresponds to an inducible p300 peak. The rows corresponding to selected PWMs are shown (please refer to Table S2 for the complete data). The overrepresented PWMs are shown as a heat plot after hierarchical clustering. The color gradient indicates the likelihood ratio (from Clover analysis) describing the probability that each p300 peak contains a given PWM (with random sets for comparison).

(C) Binding of PU.1 to selected p300-associated regions was measured by ChIP-Q-PCR. Data are expressed as percent of the input. Numbers below the columns indicate the peak ID according to Table S1. Error bars represent mean ± SEM.

(D) Effect of mutations of PU.1 binding sites on enhancer activity in luciferase assays. Three enhancers containing PU.1 sites (numbered according to Table S1) were mutagenized. Error bars represent mean ± SEM.

and 43,243 peaks in LPS-treated cells (Table S3). Using ChIP-QPCR on a group of peaks representative of a broad range of p values, we confirmed ChIP-Seq data in 95.8% of cases (23/24; Figure S3A). The two data sets overlapped by more than 84%, indicating that PU.1 binding is mainly constitutive and unaffected by stimulation (although at some regions PU.1 association was enhanced by LPS). A total of 24,791 out of the 44,445 PU.1 peaks in the untreated sample (55.8%) scored positive for all three PU.1 PWMs at high stringency, whereas 42,993 peaks (96.7%) contained at least one of them, demonstrating both the reliability of the ChIP-Seq data and the fact that recruitment occurs via direct binding to DNA. PU.1 peaks were frequently associated with intragenic (39% introns and 4% exons) and extragenic regions (37%); promoters and sequences surrounding TSSs accounted for the remaining 20% of PU.1 peaks (Figure 5A). For the subsequent analyses, peaks associated with promoters and TSSs (TSS ± 2.5 kb) were filtered out. 49.2% of inducible p300 peaks (1157/2350) in our data set overlapped distal PU.1 peaks at 2 hr (at the restrictive threshold of $p < 10^{-10}$), thus indicating that many sites of inducible p300 binding, in addition to containing binding sites for inducible but non-cell-type-restricted TFs such as NF-kB and IRF, are constitutively associated with a macrophage-restricted TF such as PU.1. In other words, PU.1 seems to constitutively mark genomic regions for inducible binding of LPS-activated TFs and p300. NF-kB was indeed recruited in a stimulus-regulated manner to regions showing constitutive PU.1 binding (Figure S3B). Representative screenshots are shown in Figure 5B

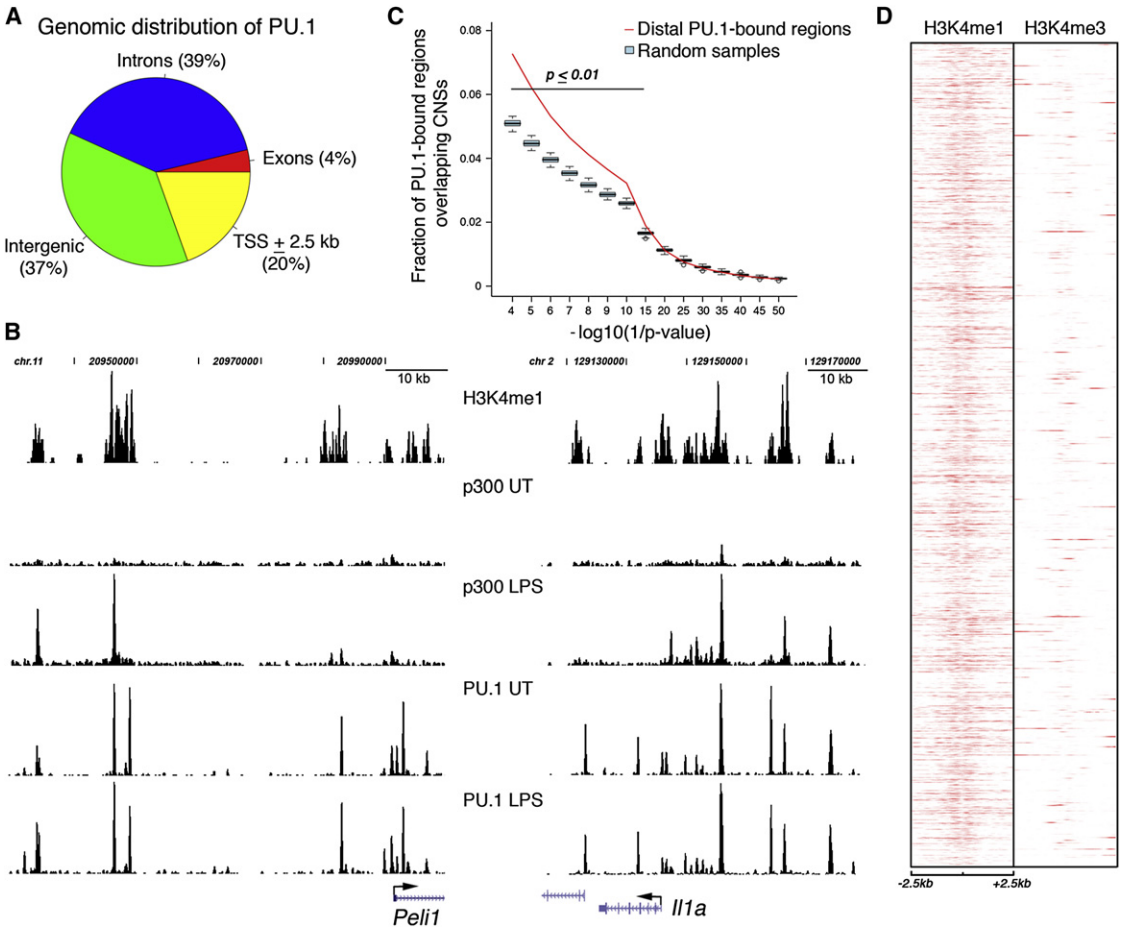

Figure 5. The Macrophage-Specific Transcription Factor PU.1 Is Constitutively Bound to Enhancers

(A) Distribution of PU.1 peaks relative to UCSC known genes.

(B) Two representative screenshots showing H3K4me1, inducible p300 binding, and constitutive PU.1 peaks.

(C) Overlap of PU.1 peaks with previously annotated CNSs. The graph shows the fraction of PU.1 peaks in untreated macrophages (red line) and random sequences (boxes) overlapping annotated CNSs (ordered by increasing p values according to Prabhakar et al., 2006).

(D) Association of PU.1 peaks with regions with a chromatin signature of enhancers. The PU.1 data set from untreated cells was overlapped with the H3K4me1 and H3K4me3 data sets. Each line represents a PU.1 peak. Peaks were ordered according to chromosomal position, from chr1 (top) to chrX (bottom) without prior clustering. Regions (5 kb) were centered on the summit of the PU.1 peaks.

and Figure S3C. Analysis of sequence conservation relative to a database of CNSs (Prabhakar et al., 2006) indicates that more than 2500 PU.1-bound, TSS-distal intra- and intergenic regions are obviously constrained, a frequency that is much higher than expected for randomly selected sequences (Figure 5C). As for p300, ultraconserved elements were not enriched in the PU.1 data set.

We also analyzed TFBS enrichment in the genomic regions corresponding to 1193 (out of 2350) distal p300 peaks that did not overlap PU.1 (Figure S4A). This group was strongly enriched for PWMs for inflammatory TFs (NF-kB, IRF, STAT1, and AP-1), as well as for lineage-restricted or fate-determining TFs such as MAFB and RUNX1 (AML1) (Figure S4A). However, only one of the three PU.1 PWMs was retrieved, indicative of a comparatively lower enrichment and/or affinity of potential PU.1 sites in this group. Indeed, when the statistical threshold for PU.1 peak calling was lowered (from 10^{-10} to 10^{-5}), 260 additional regions in this group were found to be associated to PU.1. The existence of a number of regulatory regions not associated with PU.1, however, suggests that additional lineage-specific TFs (such as MAFB) probably contribute to the genomic regulatory landscape in macrophages.

We next tested whether the H3K4me1^{hi}/H3K4me3^{lo} signature is enriched among all the distal (intergenic and intragenic) PU.1-bound regions (which largely exceed the regions associated with inducible p300 binding). Most non-promoter-associated PU.1 peaks were contained within H3K4me1^{hi}/H3K4me3^{lo} domains, thus confirming that PU.1 is preferentially associated with enhancers in macrophages (Figure 5D). In conclusion, constitutive PU.1 binding in macrophages defines dozens of thousands of regions with a genomic distribution, chromatin signature, and evolutionary constraints compatible with their function as enhancers. The strong preference of a constitutively expressed, lineage-determining TF like PU.1 for enhancers may contribute to explain the cell-type specificity of enhancer-associated function (Heintzman et al., 2009). In keeping with this notion,

enhancer sequences bound by PU.1 in macrophages were not PU.1-associated in B lymphocytes and in hematopoietic progenitors (Figure S5).

According to the data described above, regions of inducible p300 binding define a subgroup of PU.1-associated enhancers. Such regions, when searched against background sets of random genomic sequences, are enriched in binding sites for inflammatory TFs (see Figure 4B). Therefore we examined whether they are also different from the pool of all distal PU.1-bound regions in terms of TFBS composition. When the distal PU.1 peaks were used as a background set, the inducible p300 data set was enriched for NF-κB, IRF, and FOS-AP1 sites (Figure S4B and Table S4), indicating that inducible p300 binding identifies a subgroup of PU.1-associated enhancers that is specifically enriched in binding sites for essential inflammatory TFs.

An Active Role for PU.1 in Enhancer Organization

The extensive overlap between PU.1 and enhancers in macrophages suggests the possibility that PU.1 may directly impart properties of enhancers to the genomic regions to which it is recruited. To directly test this possibility, we first analyzed the effects of PU.1 depletion in primary macrophages. Although global H3K4me1 amounts were unaffected, several enhancers in both the inducible and noninducible groups showed various degrees of H3K4me1 reduction (Figures 6A and 6B). Lack of effects on other enhancers may reflect redundancy or, more trivially, the activity of the residual amount of PU.1 in depleted cells (Figure 6C). Given these data, we considered the possibility that ectopic expression of PU.1 may drive de novo formation of enhancers in nonhematopoietic cells, which would be consistent with the reported ability of PU.1 to partially convert fibroblasts into macrophages (Feng et al., 2008). As described, retroviral expression of PU.1 in 3T3 cells was sufficient to induce the upregulation of some macrophage-restricted genes (Figure 6D) like *Cd68*, *Emr1*, and *Lyz2*, some of them being much stronger induced upon coexpression of C/EBPα (Feng et al., 2008) (data not shown). Ectopically expressed PU.1 bound to genomic regions corresponding to macrophage enhancers (Figure 6E), and recruitment was associated with a several-fold increase in H3K4me1 (Figure 6F). Moreover, the regions bound by PU.1 upon overexpression in 3T3 cells acquired properties of nucleosome-depleted chromatin similar to those constitutively shown by the same regions in macrophages (Figures 6G and 6H). This latter result indicates that nucleosome depletion in enhancers (Figure 2 and Figure S2) is caused, and maintained by, constitutive TF binding (rather than representing a default state caused by the inability of these sequences to assemble nucleosomes).

DISCUSSION

The recent identification of a chromatin signature characteristic of enhancers, together with the recognition that enhancers are bound by histone acetyltransferases (Heintzman et al., 2007), enabled large-scale approaches to enhancer mapping in multiple cell types (Heintzman et al., 2009; Visel et al., 2009). However, unraveling the complex repertoire of enhancers present in a given cell type ("enhanceomes") in order to identify functionally homogeneous discrete subgroups active in specific responses is still a major challenge. Moreover, apart from anecdotal descriptions, the genomic determinants of enhancer function are still largely unknown.

The objective of this study was the identification of the organizational principles of enhancers controlling a prototypical environmental response influenced by the cellular context, namely the endotoxin-induced inflammatory gene expression program in macrophages. Our data showed that LPS-inducible binding of p300 to chromatin can be exploited to identify enhancers associated with inducible genes. Analysis of the underlying genomic sequences allowed us to find a common, intuitive and highly rational regulatory logic, consisting in the combination of binding sites for one or more cell-type restricted and constitutive TFs (particularly PU.1, but also MAFB and RUNX1) with binding sites for ubiquitous and stimulus-activated TFs like NF-kB, IRF, and AP1. We suggest that this organization allows the response induced by inflammatory stimuli to be adapted to the specific cellular context in which it is elicited. We envision that this architectural principle may hold true also for enhancers involved in other types of stress responses. Moreover, the requirement for PU.1 for maintenance of H3K4me1 at several enhancers in macrophages, and its ability to locally increase H3K4me1 and accessibility upon ectopic expression, suggests that PU.1 may be both required and sufficient to functionalize genomic regions as enhancers. This property may explain its ability to convert fibroblasts into macrophages (Feng et al., 2008), and more in general allows hypothesizing that several fate-determining TFs may rewire transcriptional circuits largely by inducing formation of novel enhancers. Because PU.1 extensively marks active promoters in addition to enhancers, and because distant regulatory regions are brought in physical proximity to promoters and TSSs by looping out the intervening genomic regions, an exciting scenario is that PU.1 may pervasively contribute to shape the 3D landscape of the macrophage genome, in fact acting as a global genomic organizer.

The data described here also raise two groups of questions. First, what are the regulatory genomic regions involved in the transcriptional response to the same stimulus (LPS) in cell types other than macrophages? Our model suggests that functionalization of specific genomic regions as enhancers depends on tissue-restricted TFs like PU.1, which are characterized by a capillary genomic distribution and the ability to generate nucleosome-free, accessible stretches of DNA sequence: therefore, a prediction of the model is that in other cell types, the regulatory landscape will be determined and maintained by TFs with a different genomic distribution, leading to the usage of distinct genomic regions in response to the same stimulus. Alternative usage of the available regulatory information contained in the genome when different cells are exposed to the same stimulus would represent the molecular basis for specialized responses to identical environmental inputs. Second, how do unrelated inflammatory stimuli (e.g., TNF or IL1) exploit the regulatory genomic information within the global landscape provided by PU.1 (or equivalent master regulators in different cell types)? The simplest possibility is that usage of the vast array of available regulatory regions (that are kept functional and accessible by PU.1) will largely or exclusively depend on the specific set of TFs induced or activated by each individual stimulus, thus leading to both overlapping and stimulus-specific utilization of the accessible genomic regulatory information.

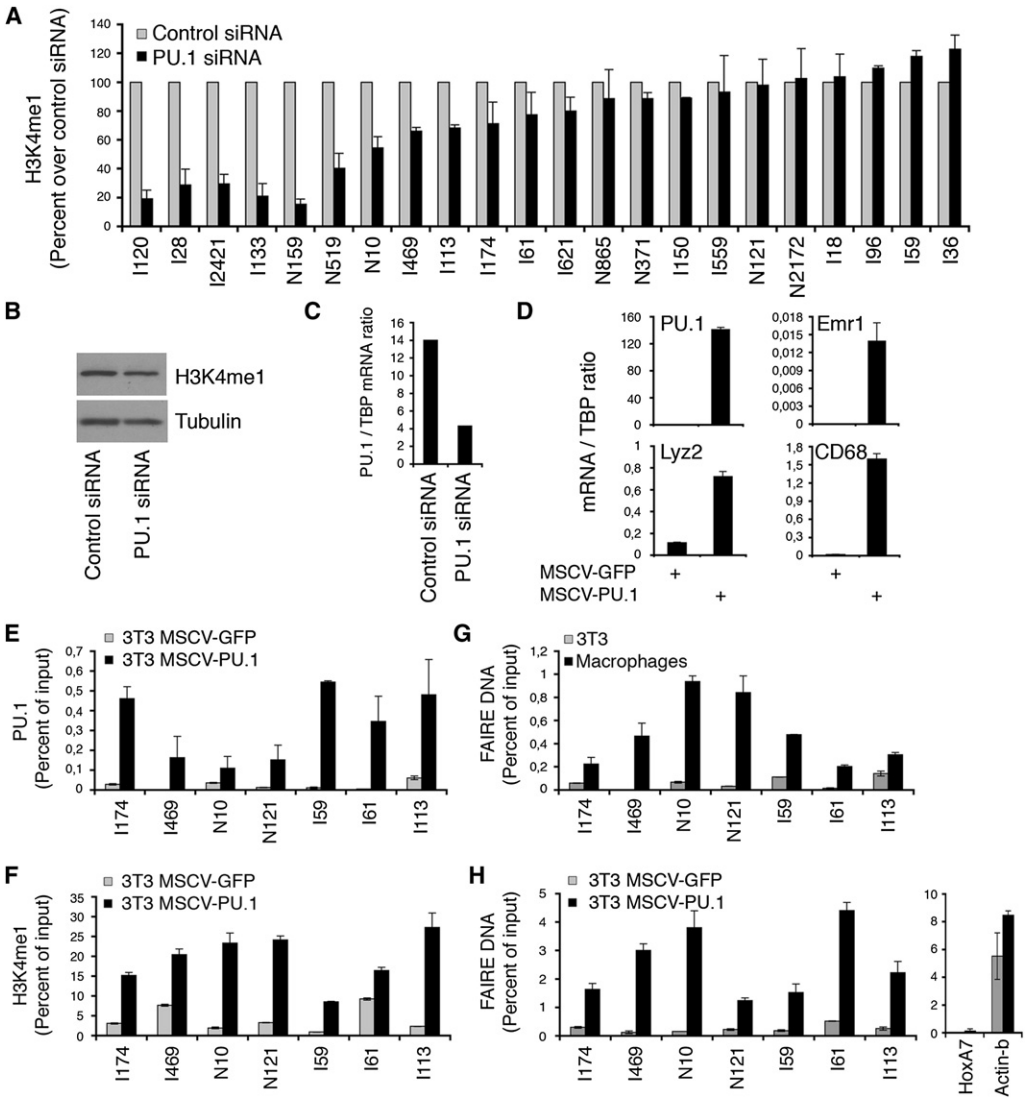

Figure 6. PU.1 Controls H3K4me1 at Its Genomic Binding Sites

(A) H3K4me1 ChIP in bone marrow-derived macrophages transfected with either a control (scrambled) siRNA or a mixture of PU.1-specific siRNAs. Data are expressed as percent of H3K4me1 measured in cells exposed to control siRNA. Peaks IDs refer to Table S1 (I, Inducible peaks; N, noninducible peaks). Error bars represent means ± SEM.

(B) Total H3K4me1 amounts in PU.1-depleted macrophages. Tubulin was used as a loading control.

(C) PU.1 expression in control and PU.1-siRNA cells were measured by Q-PCR.

(D) Retroviral expression of PU.1 in fibroblasts induces the expression of macrophage markers. Error bars represent mean ± SD.

(E) PU.1 ChIP was carried out on 3T3 fibroblasts infected with a control retrovirus (MSCV-GFP) or a PU.1-EGFP-expressing retrovirus (MSCV-PU.1). Cells were subjected to four rounds of infection over 2 days and harvested at the fifth day after the last infection. Infection efficiency was >95%. Error bars represent means ± SEM.

(F) H3K4me1 ChIP on the same samples. See Table S1 for genomic locations of the indicated peaks. Error bars: means ± SEM.

(G) FAIRE (formaldehyde-assisted isolation of regulatory elements) (Giresi et al., 2007) was used for isolating accessible, nucleosome-depleted DNA from macrophages and 3T3 cells. Error bars represent means ± SEM.

(H) FAIRE analysis on 3T3 cells infected with a control virus or with the PU.1-expressing virus. Signal is shown as percent of input. HoxA and beta-Actin promoters are non-PU.1 targets with a constitutively silent or active chromatin configuration, respectively. Error bars represent means ± SEM.

The observation that p300 is recruited to *cis*-regulatory regions in response to stimulation is unexpected in the light of previous ChIP-chip data in human transformed cell lines (Heintzman et al., 2007; Heintzman et al., 2009). In these studies it was shown that both H3K4me1 and p300 constitutively mark sites for inducible recruitment of the IFN-γ-activated TF Stat1. Although at a superficial analysis our results (and specifically the observation that p300 binding is often inducible) may appear to be in conflict with the data reported in those studies, in fact this is only partially true. First, we also detected constitutive p300 binding at regions adjacent to many inducible genes, and a fraction of the inducible p300 peaks we found could already be

detected in basal conditions. Second, in the experiments by Heintzman et al. a very short stimulation with IFN-γ was used (20 min) (Heintzman et al., 2007; Heintzman et al., 2009), implying that transcriptional events occurring with slower kinetics were overlooked. Third, regulatory circuits operating in primary, highly differentiated and specialized cells like macrophages may be lost in transformed and continuously cultured cell lines. Finally, it should be stressed that the notion that p300 can be recruited to chromatin in a stimulus-regulated manner is consistent with experimental data accumulated over several years and demonstrates that p300 is recruited to chromatin by association with TFs activated by environmental stimuli, including members of the NF-kB, IRF, and AP-1 families (Zhong et al., 1998; Hottiger et al., 1998; Merika et al., 1998; Lin et al., 1999; Kamei et al., 1996; Vanden Berghe et al., 1999; Lin et al., 2001; Wathelet et al., 1998).

In conclusion, this study demonstrates how a specific genomic organization at a functionally related group of enhancers is directly translated into function. The combination of binding sites for a cell type-restricted constitutive TF (which provide context-dependence to the response) and binding sites for ubiquitous inducible TFs (which provide responsiveness to external stimuli), probably represent a general framework for genomic regulatory regions controlling specialized reactions to external stimuli.

EXPERIMENTAL PROCEDURES

Cell Culture

Bone marrow cells isolated from female Fvb/Hsd mice were plated in 10 cm plates in 5 ml of BM-medium (high glucose DMEM supplemented with 20% lowendotoxin fetal bovine serum, 30% L929-conditioned medium, 1% glutamine, 1%, Pen/Strep, 0.5% sodium pyruvate, and 0.1% β-mercaptoethanol). Cultures were fed with 2.5 ml of fresh medium every 2 days. Stimulations were carried out at day 7. RAW 264.7 (mouse macrophage cells), Hepa 1-6 (mouse hepatoma cells), and EML (clone 1) were purchased from the American Type Culture Collection (ATCC). A20 cells were a gift from S. Casola. Cells were grown in Dulbecco minimal essential medium (DMEM) containing 10% fetal bovine serum (FBS) and 2 mM glutamine. EML1 cells were grown in the presence of SCF (100 ng/ml). C57/B1 (mouse melanoma epithelial cells) from ATCC were grown in MEM + 10% FBS supplemented with 2 mM glutamine, 1 mM sodium pyruvate, and 0.1 mM non essential amino acids (NEAA). LPS from *E. Coli* serotype EH100 (Alexis) was used at 10 ng/ml.

Chromatin Immunoprecipitation

For ChIP experiments, bone marrow macrophages were left untreated or stimulated for 2 hr with LPS. Fixation with formaldehyde and sonication was carried out as described previously (De Santa et al., 2007). p300, H3K4me1, H3K4me3, and Pu.1 ChIP lysates were generated from 2×10^8, 0.5×10^8 cells, 1×10^8, and 0.3×10^8 cells respectively. Each lysate was immunoprecipitated with 10 μg of the following antibodies: p300 (Santa Cruz sc-585), p65 (Santa Cruz sc-372), antiH3K4me1 (Abcam Ab8895), antiH3K4me3 (Abcam Ab8580), and PU.1 (Santa Cruz sc-352).

Antibodies were prebound overnight to 100 μl of G protein-coupled paramagnetic beads (Dynabeads) in PBS/BSA 0.5%. Beads were then added to lysates (the preclearing step was omitted), and incubation was allowed to proceed overnight. Beads were washed six times in a modified RIPA buffer (50 mM HEPES [pH 7.6], 500 mM LiCl, 1 mM EDTA, 1% NP-40, and 0.7% Na-deoxycholate) and once in TE containing 50 mM NaCl. DNA was eluted in TE containing 2% SDS and crosslinks reversed by incubation overnight at 65°C. DNA was then purified by Qiaquick columns (QIAGEN) and quantified with PicoGreen (Invitrogen). Yields were ~10 ng/10^8 cells (p300), ~200 ng/10^8 cells (H3K4me1), ~300 ng/10^8 cells (H3K4me3), and ~250 ng/10^8 cells (Pu.1). For p300, two independent biological replicates were used. For validation by ChIP-QPCR, 1 μl of purified DNA was used for amplified on an Applied Biosystems 7500 Fast Real-time PCR system (with Applied Biosystem Sybrgreen). Primers used for ChIP QPCR are in Table S5.

Preparation of ChIP DNA Libraries, Sequencing, and Computational Analysis

A detailed description of the ChIP-Sequencing methods and the computational analyses is provided in the Supplemental Experimental Procedures. Statistics referring to the sequencing runs are in Table S6.

Transient Transfections, Reporter Assays, RNAi, and Retroviral Infections

RAW264.7, Hepa 1-6, and C57/B1 cells were transiently transfected in a 24-well format with 0.8 μg of empty vector (pGL3-promoter vector, Promega) or vectors containing the specified genomic regions (Table S5) with Lipofectamine 2000 (Invitrogen) in accordance with the manufacturer's protocol. Twenty-four hours after transfection, cells were treated with LPS (10 ng/ml), and luciferase assay (Bright-Glo Luciferase Assay System, Promega) was performed 16 hr after treatment. Values are expressed as n-fold increase in luciferase counts over the empty vector for each cell line. For siRNA experiments, bone marrow-derived macrophages were transfected with control or smartpool siRNAs (100 nM, Dharmacon) directed against PU.1 with lipofectamine 2000 (Invitrogen). Cells were used for ChIP experiments after 48 hr, and target gene knockdown was validated by QPCR. 3T3 cells (a gift from Alex Hoffman, UCSD) were infected with MSCV-IRES-GFP or MSCV-IRES-PU.1-GFP, as described (Feng et al., 2008). Cells underwent four cycles of infection over 2 days and were collected 5 days after the last infection. For the FAIRE (Formaldehyde-Assisted Isolation of Regulatory Elements) experiment (Giresi et al., 2007), cells were crosslinked and sonicated as for ChIP experiments. DNA from bone marrow macrophages (1×10^8 cells), 3T3 cells (1×10^8 cells), 3T3 infected with MSCV-IRES-GFP, or MSCV-IRES-PU.1-GFP (1×10^7 cells) was isolated by addition of an equal volume of phenol-chloroform. Before extraction, 50 μl of the lysate were kept as input. The aqueous phase was isolated and both inputs and samples were subjected to cross-link reversal at 65°C overnight after addition of SDS. DNA was then purified with Qiaquick columns and subjected to QPCR analysis.

ACCESSION NUMBERS

The ChIP-Seq data sets are available in the Gene Expression Omnibus (GEO) database (http://www.ncbi.nlm.nih.gov/gds) under the accession number GSE19553.

SUPPLEMENTAL INFORMATION

Supplemental Information includes six figures, six tables, and Supplemental Experimental Procedures and can be found with this article online at doi:10.1016/j.immuni.2010.02.008.

ACKNOWLEDGMENTS

This work was supported by the FP6 and FP7 programs of the European Community (Marie Curie Excellence Grant Trans-Tar to GN; Model-In consortium to G.N. and J.R.); the Italian Association for Research on Cancer, AIRC (G.N.); a donation from Manetti & Roberts and the Fondazione Umberto Veronesi (to G.N.); the NIH ENCODE grant 1R01HG003521-01 (C.L.W.) and the Agency for Science, Technology and Research (A*STAR) of Singapore. We thank B. Amati and F. Ciccarelli (IEO) for comments on the manuscript; T. Graf (CRG, Barcelona) for the PU.1 retroviral expression vectors; the Next Generation Sequencing Team at the Cogentech Consortium (IFOM-IEO Campus) and the sequencing team at GIS for the generation of the ChIP-Seq data; M. Cesaroni, L. Fornasari, and G. Gargiulo (IEO) for useful discussions on data analysis. S.G. carried out the H3K4me1 and p300 ChIP-Seq experiments, their validation and the functional assays with the help of S.P. I.B. carried out all computational analyses. F.M. carried out the PU.1 ChIP-Seq and its validation and the PU.1 over-expression experiment in 3T3. F.D.S. generated the H3K4me3 data set in collaboration with A.C. and the C.L.W. group. E.V., L.L. and L.G. prepared and ran the ChIP-Seq samples.

J.R. supervised the generation of the H3K4me1 data set. GN designed the study and wrote the paper.

Received: January 7, 2010
Revised: February 3, 2010
Accepted: February 4, 2010
Published online: March 4, 2010

REFERENCES

Badis, G., Berger, M.F., Philippakis, A.A., Talukder, S., Gehrke, A.R., Jaeger, S.A., Chan, E.T., Metzler, G., Vedenko, A., Chen, X., et al. (2009). Diversity and complexity in DNA recognition by transcription factors. Science *324*, 1720–1723.

Baud, V., and Karin, M. (2001). Signal transduction by tumor necrosis factor and its relatives. Trends Cell Biol. *11*, 372–377.

Bejerano, G., Pheasant, M., Makunin, I., Stephen, S., Kent, W.J., Mattick, J.S., and Haussler, D. (2004). Ultraconserved elements in the human genome. Science *304*, 1321–1325.

Birney, E., Stamatoyannopoulos, J.A., Dutta, A., Guigó, R., Gingeras, T.R., Margulies, E.H., Weng, Z., Snyder, M., Dermitzakis, E.T., Thurman, R.E., et al. ENCODE Project Consortium, NISC Comparative Sequencing Program, Baylor College of Medicine Human Genome Sequencing Center, Washington University Genome Sequencing Center, Broad Institute, Children's Hospital Oakland Research Institute (2007). Identification and analysis of functional elements in 1% of the human genome by the ENCODE pilot project. Nature *447*, 799–816.

Boffelli, D., McAuliffe, J., Ovcharenko, D., Lewis, K.D., Ovcharenko, I., Pachter, L., and Rubin, E.M. (2003). Phylogenetic shadowing of primate sequences to find functional regions of the human genome. Science *299*, 1391–1394.

Carninci, P., Sandelin, A., Lenhard, B., Katayama, S., Shimokawa, K., Ponjavic, J., Semple, C.A., Taylor, M.S., Engström, P.G., Frith, M.C., et al. (2006). Genome-wide analysis of mammalian promoter architecture and evolution. Nat. Genet. *38*, 626–635.

De Santa, F., Totaro, M.G., Prosperini, E., Notarbartolo, S., Testa, G., and Natoli, G. (2007). The histone H3 lysine-27 demethylase Jmjd3 links inflammation to inhibition of polycomb-mediated gene silencing. Cell *130*, 1083–1094.

De Santa, F., Narang, V., Yap, Z.H., Tusi, B.K., Burgold, T., Austenaa, L., Bucci, G., Caganova, M., Notarbartolo, S., Casola, S., et al. (2009). Jmjd3 contributes to the control of gene expression in LPS-activated macrophages. EMBO J. *28*, 3341–3352.

DeKoter, R.P., and Singh, H. (2000). Regulation of B lymphocyte and macrophage development by graded expression of PU.1. Science *288*, 1439–1441.

Doyle, S., Vaidya, S., O'Connell, R., Dadgostar, H., Dempsey, P., Wu, T., Rao, G., Sun, R., Haberland, M., Modlin, R., and Cheng, G. (2002). IRF3 mediates a TLR3/TLR4-specific antiviral gene program. Immunity *17*, 251–263.

Eichbaum, Q.G., Iyer, R., Raveh, D.P., Mathieu, C., and Ezekowitz, R.A. (1994). Restriction of interferon gamma responsiveness and basal expression of the myeloid human Fc gamma R1b gene is mediated by a functional PU.1 site and a transcription initiator consensus. J. Exp. Med. *179*, 1985–1996.

Feng, R., Desbordes, S.C., Xie, H., Tillo, E.S., Pixley, F., Stanley, E.R., and Graf, T. (2008). PU.1 and C/EBPalpha/beta convert fibroblasts into macrophage-like cells. Proc. Natl. Acad. Sci. USA *105*, 6057–6062.

Giresi, P.G., Kim, J., McDaniell, R.M., Iyer, V.R., and Lieb, J.D. (2007). FAIRE (Formaldehyde-Assisted Isolation of Regulatory Elements) isolates active regulatory elements from human chromatin. Genome Res. *17*, 877–885.

Grove, M., and Plumb, M. (1993). C/EBP, NF-kappa B, and c-Ets family members and transcriptional regulation of the cell-specific and inducible macrophage inflammatory protein 1 alpha immediate-early gene. Mol. Cell. Biol. *13*, 5276–5289.

Hayden, M.S., and Ghosh, S. (2008). Shared principles in NF-kappaB signaling. Cell *132*, 344–362.

Hayden, M.S., West, A.P., and Ghosh, S. (2006). NF-kappaB and the immune response. Oncogene *25*, 6758–6780.

Heintzman, N.D., Stuart, R.K., Hon, G., Fu, Y., Ching, C.W., Hawkins, R.D., Barrera, L.O., Van Calcar, S., Qu, C., Ching, K.A., et al. (2007). Distinct and predictive chromatin signatures of transcriptional promoters and enhancers in the human genome. Nat. Genet. *39*, 311–318.

Heintzman, N.D., Hon, G.C., Hawkins, R.D., Kheradpour, P., Stark, A., Harp, L.F., Ye, Z., Lee, L.K., Stuart, R.K., Ching, C.W., et al. (2009). Histone modifications at human enhancers reflect global cell-type-specific gene expression. Nature *459*, 108–112.

Hottiger, M.O., Felzien, L.K., and Nabel, G.J. (1998). Modulation of cytokine-induced HIV gene expression by competitive binding of transcription factors to the coactivator p300. EMBO J. *17*, 3124–3134.

Jones, P.L., Ping, D., and Boss, J.M. (1997). Tumor necrosis factor alpha and interleukin-1beta regulate the murine manganese superoxide dismutase gene through a complex intronic enhancer involving C/EBP-beta and NF-kappaB. Mol. Cell. Biol. *17*, 6970–6981.

Kamei, Y., Xu, L., Heinzel, T., Torchia, J., Kurokawa, R., Gloss, B., Lin, S.C., Heyman, R.A., Rose, D.W., Glass, C.K., and Rosenfeld, M.G. (1996). A CBP integrator complex mediates transcriptional activation and AP-1 inhibition by nuclear receptors. Cell *85*, 403–414.

Katzman, S., Kern, A.D., Bejerano, G., Fewell, G., Fulton, L., Wilson, R.K., Salama, S.R., and Haussler, D. (2007). Human genome ultraconserved elements are ultraselected. Science *317*, 915.

Kelly, L.M., Englmeier, U., Lafon, I., Sieweke, M.H., and Graf, T. (2000). MafB is an inducer of monocytic differentiation. EMBO J. *19*, 1987–1997.

Lin, R., Heylbroeck, C., Genin, P., Pitha, P.M., and Hiscott, J. (1999). Essential role of interferon regulatory factor 3 in direct activation of RANTES chemokine transcription. Mol. Cell. Biol. *19*, 959–966.

Lin, C.H., Hare, B.J., Wagner, G., Harrison, S.C., Maniatis, T., and Fraenkel, E. (2001). A small domain of CBP/p300 binds diverse proteins: Solution structure and functional studies. Mol. Cell *8*, 581–590.

Merika, M., Williams, A.J., Chen, G., Collins, T., and Thanos, D. (1998). Recruitment of CBP/p300 by the IFN beta enhanceosome is required for synergistic activation of transcription. Mol. Cell *1*, 277–287.

Nagamura-Inoue, T., Tamura, T., and Ozato, K. (2001). Transcription factors that regulate growth and differentiation of myeloid cells. Int. Rev. Immunol. *20*, 83–105.

Nerlov, C., and Graf, T. (1998). PU.1 induces myeloid lineage commitment in multipotent hematopoietic progenitors. Genes Dev. *12*, 2403–2412.

Nguyen, V.T., and Benveniste, E.N. (2000). Involvement of STAT-1 and ets family members in interferon-gamma induction of CD40 transcription in microglia/macrophages. J. Biol. Chem. *275*, 23674–23684.

Pennacchio, L.A., Ahituv, N., Moses, A.M., Prabhakar, S., Nobrega, M.A., Shoukry, M., Minovitsky, S., Dubchak, I., Holt, A., Lewis, K.D., et al. (2006). In vivo enhancer analysis of human conserved non-coding sequences. Nature *444*, 499–502.

Ponting, C.P. (2008). The functional repertoires of metazoan genomes. Nat. Rev. Genet. *9*, 689–698.

Prabhakar, S., Poulin, F., Shoukry, M., Afzal, V., Rubin, E.M., Couronne, O., and Pennacchio, L.A. (2006). Close sequence comparisons are sufficient to identify human cis-regulatory elements. Genome Res. *16*, 855–863.

Ramirez-Carrozzi, V.R., Braas, D., Bhatt, D.M., Cheng, C.S., Hong, C., Doty, K.R., Black, J.C., Hoffmann, A., Carey, M., and Smale, S.T. (2009). A unifying model for the selective regulation of inducible transcription by CpG islands and nucleosome remodeling. Cell *138*, 114–128.

Sandelin, A., Alkema, W., Engström, P., Wasserman, W.W., and Lenhard, B. (2004). JASPAR: An open-access database for eukaryotic transcription factor binding profiles. Nucleic Acids Res. *32* (*Database issue*), D91–D94.

Sanjabi, S., Hoffmann, A., Liou, H.C., Baltimore, D., and Smale, S.T. (2000). Selective requirement for c-Rel during IL-12 P40 gene induction in macrophages. Proc. Natl. Acad. Sci. USA *97*, 12705–12710.

Scott, E.W., Simon, M.C., Anastasi, J., and Singh, H. (1994). Requirement of transcription factor PU.1 in the development of multiple hematopoietic lineages. Science *265*, 1573–1577.

Siepel, A., Bejerano, G., Pedersen, J.S., Hinrichs, A.S., Hou, M., Rosenbloom, K., Clawson, H., Spieth, J., Hillier, L.W., Richards, S., et al. (2005). Evolutionarily conserved elements in vertebrate, insect, worm, and yeast genomes. Genome Res. *15*, 1034–1050.

Taniguchi, T., Ogasawara, K., Takaoka, A., and Tanaka, N. (2001). IRF family of transcription factors as regulators of host defense. Annu. Rev. Immunol. *19*, 623–655.

Tracey, K.J., and Cerami, A. (1994). Tumor necrosis factor: A pleiotropic cytokine and therapeutic target. Annu. Rev. Med. *45*, 491–503.

Vanden Berghe, W., De Bosscher, K., Boone, E., Plaisance, S., and Haegeman, G. (1999). The nuclear factor-kappaB engages CBP/p300 and histone acetyltransferase activity for transcriptional activation of the interleukin-6 gene promoter. J. Biol. Chem. *274*, 32091–32098.

Visel, A., Prabhakar, S., Akiyama, J.A., Shoukry, M., Lewis, K.D., Holt, A., Plajzer-Frick, I., Afzal, V., Rubin, E.M., and Pennacchio, L.A. (2008). Ultraconservation identifies a small subset of extremely constrained developmental enhancers. Nat. Genet. *40*, 158–160.

Visel, A., Blow, M.J., Li, Z., Zhang, T., Akiyama, J.A., Holt, A., Plajzer-Frick, I., Shoukry, M., Wright, C., Chen, F., et al. (2009). ChIP-seq accurately predicts tissue-specific activity of enhancers. Nature *457*, 854–858.

Wathelet, M.G., Lin, C.H., Parekh, B.S., Ronco, L.V., Howley, P.M., and Maniatis, T. (1998). Virus infection induces the assembly of coordinately activated transcription factors on the IFN-beta enhancer in vivo. Mol. Cell *1*, 507–518.

Zhong, H., Voll, R.E., and Ghosh, S. (1998). Phosphorylation of NF-kappa B p65 by PKA stimulates transcriptional activity by promoting a novel bivalent interaction with the coactivator CBP/p300. Mol. Cell *1*, 661–671.